

Review

## Luminescent Oxygen Gas Sensors Based on Nanometer-Thick Hybrid Films of Iridium Complexes and Clay Minerals

Hisako Sato <sup>1,\*†</sup>, Kenji Tamura <sup>2,†</sup> and Akihiko Yamagishi <sup>3,†</sup>

<sup>1</sup> Department of Chemistry, Graduate School of Science and Engineering, Ehime University, Matsuyama 790-8577, Japan

<sup>2</sup> National Institute for Materials Science, Tsukuba 305-0044, Japan;  
E-Mail: TAMURA.Kenji@nims.go.jp

<sup>3</sup> School of Medicine, Toho University, Ota-ku, Tokyo 143-8540, Japan;  
E-Mail: akihiko.yamagishi@sci.toho-u.ac.jp

† These authors contributed equally to this work.

\* Author to whom correspondence should be addressed; E-Mail: sato.hisako.my@ehime-u.ac.jp;  
Tel.: +81-89-927-9599; Fax: +81-89-927-9590.

Received: 25 November 2013; in revised form: 27 December 2013 / Accepted: 6 January 2014 /  
Published: 17 January 2014

---

**Abstract:** The use of Ir(III) complexes in photo-responsive molecular devices for oxygen gas sensing is reviewed. Attention is focused on the immobilization of Ir(III) complexes in organic or inorganic host materials such as polymers, silica and clays in order to enhance robustness and reliability. Our recent works on constructing nanometer-thick films comprised of cyclometalated cationic Ir(III) complexes and clay minerals are described. The achievement of multi-emitting properties in response to oxygen pressure is demonstrated.

**Keywords:** clay mineral; Langmuir-Blodgett film; cyclometalated iridium complex; phosphorescence; oxygen; gas sensing; quenching; energy transfer

---

### 1. Introduction

There has been extensive interest in developing photo-responsive solid-state chemical sensor devices based on luminescent transition metal complexes [1–5]. Cyclometalated iridium(III) complexes (denoted by Ir(III)) are a promising applicant for emitting elements due to their high

emitting properties in a visible region [6–15]. They are characterized by the long lifetime of excited triplet states and the high quantum yield of emission. Ir(III) complexes are used for photo-responsive molecular devices such as LED devices and oxygen sensors [16–34].

The quantitative determination of oxygen concentration is essential to various fields ranging from life sciences to environmental applications. The applicability of Ir(III) complexes for this purpose is based on the premise that energy transfer takes place efficiently from the triplet excited state of an Ir(III) complex to an oxygen molecule in a triplet ground state [30]. In order to enhance robustness and reliability of sensing devices, Ir(III) complexes are often immobilized into organic or inorganic host materials such as polymers, silica and clay minerals [35–51]. The inclusion of an Ir(III) complex, for example, [Ir(2-phenylpyridine)<sub>2</sub>(4,4'-bis(2-(4-*N,N*-methylhexylaminophenyl)ethyl)-2,2'-bipyridine)]Cl in polymer matrices has been reported for probing oxygen molecules [43]. The sensitivity of the Ir(III) complex was enhanced when it was immobilized in polymers such as polystyrene. The constructed films showed long-term stability and the complete reversibility of signals quenched by oxygen and quick response time to various oxygen concentrations. In contrast to these hybridization attempts, the luminescent Langmuir-Blodgett (LB) films of pure Ir(III) complexes were recently prepared by depositing a floating monolayer of an amphiphilic Ir(III) complex onto a solid substrate in order to fabricate a thin film sensor [35–39].

Among attempts to immobilize Ir(III) complexes, clay minerals have been used as an inorganic host with two-dimensional periodicity [50–65]. The photo-responsive solid-state gas sensors are manipulated on the basis of the thin film preparation of clay minerals. According to the method, hybridization took place electrostatically between a cationic monolayer and negatively charged clay particles (clay nonosheets) at an air–water interface (the so-called “*Clay Langmuir-Blodgett (LB) Method*”) [39].

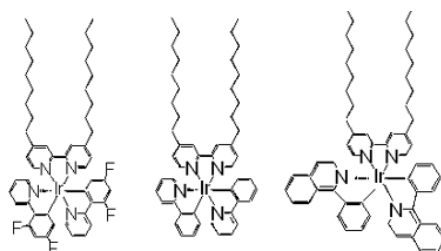
In the present review, we describe recent attempts of fabricating hybrid LB films of Ir(III) complexes with clay minerals [39,66–68]. Ir(III) complexes with different emission colors (e.g., blue, green and red emissions) were used. Films were constructed by the layer-by-layer deposition of floating hybrid films onto a hydrophilic quartz substrate. When emission spectra were measured in vacuum or under oxygen atmosphere, it was revealed that the efficiency of energy transfer was critically dependent on *the deposition order* of incorporated Ir(III) complexes; this led to the appearance of the clear color change in emission, in response to oxygen pressure. These properties would be useful not only for detection but also for rapid visual response. The work would become a benchmark to explore a multi-emitting solid-state gas sensor film based on cyclometalated iridium(III) complexes.

## **2. Preparation of the Thin Films of Clay Minerals by the Modified Langmuir-Blodgett (LB) Method**

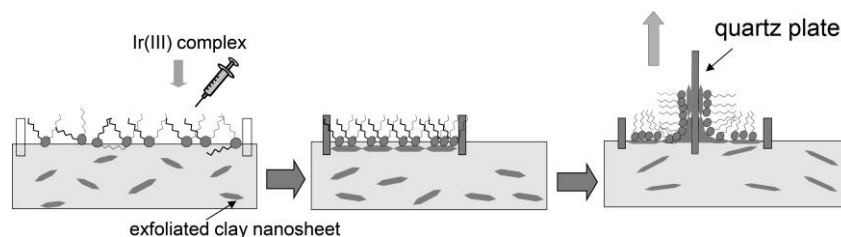
Clay minerals are known to act as host intercalating photoresponsive molecules [50–67]. Recently the photochemical reactions involving clay minerals were further extended to thin film systems. In previous attempts, for example, the extent of energy transfer between donor and acceptor molecules in different layers was estimated [35,52,66,67]. We have employed clay minerals as a host of Ir(III) complexes. In such attempts, the preparation of thin films with uniform thickness is essentially important to achieve well-defined sensing systems. To fabricate films of high quality, the following

amphiphilic cyclometalated iridium(III) complexes (Ir(III)) with different emission characters were used:  $[\text{Ir}(\text{ppy})_2(\text{dc18bpy})]^+$  ( $\text{ppy} = 2\text{-phenylpyridine}$ ;  $\text{dc18bpy} = 4,4'\text{-dioctadecyl-2,2'-bipyridine}$ ),  $[\text{Ir}(\text{dfppy})_2(\text{dc9bpy})]^+$  ( $\text{fppyH} = 2\text{-}(4',6'\text{-difluorophenyl})\text{pyridine}$ ;  $\text{dc9bpy} = 4,4'\text{-dinonyl-2,2'-bipyridine}$ ) (denoted by DFPPY),  $[\text{Ir}(\text{ppy})_2(\text{dc9bpy})]^+$  (denoted by PPY) and or  $[\text{Ir}(\text{piq})_2(\text{dc9bpy})]^+$  ( $\text{piqH} = 1\text{-phenyisoquinoline}$  (denoted by PIQ)). Their molecular structures are shown in Chart 1. The modified Langmuir-Blodgett (LB) method (“Clay LB Method”) has been applied for preparing a thin clay film according to the procedures shown in Scheme 1.

**Chart 1.** (left)  $[\text{Ir}(\text{dfppy})_2(\text{dc9bpy})]^+$  ( $\text{fppyH} = 2\text{-}(4',6'\text{-difluorophenyl})\text{pyridine}$ ;  $\text{dc9bpy} = 4,4'\text{-dinonyl-2,2'-bipyridine}$ ) (denoted by DFPPY), (middle)  $[\text{Ir}(\text{ppy})_2(\text{dc9bpy})]^+$  (denoted by PPY) and (right)  $[\text{Ir}(\text{piq})_2(\text{dc9bpy})]^+$  ( $\text{piqH} = 1\text{-phenyisoquinoline}$  (denoted by PIQ)).



**Scheme 1.** Modified Langmuir-Blodgett (LB) method (“Clay LB Method”) (modified from reference [69]).



“Clay LB Method” was first reported when the nanometer-thick film of an ion-exchange adduct of a clay (synthetic saponite) was prepared by hybridizing an amphiphilic alkylammonium cation (trimethylstearylammmonium) with an exfoliated sheet of clay minerals [69]. According to the method, the floating monolayer of an amphiphilic cation was formed onto a subphase of an aqueous suspension of clay minerals. Negatively charged clay nanosheets were attached onto the tail side of the floating monolayer. A layer-by-layer deposited film was prepared by transferring such a hybrid film onto a solid substrate by the Langmuir-Blodgett (LB) method. Extending the method to heterogeneous multilayered films, different kinds of cationic molecules were intercalated in a controlled order. It was revealed that a single clay layer acted as an efficient barrier in the stereoselective transfer of photon energy [69].

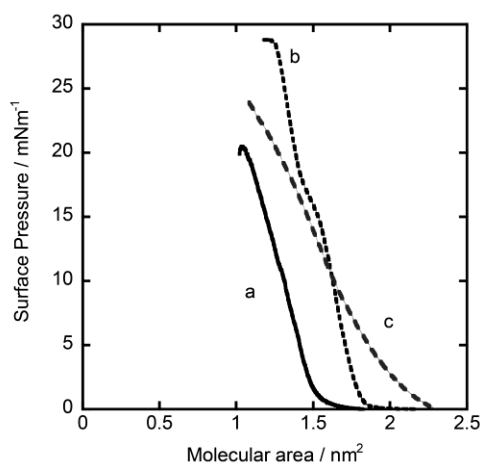
We optimized the conditions of preparing Ir(III)-clay hybrid films with high quality. A LB trough with an area of  $10.0\text{ cm} \times 13.0\text{ cm}$  was maintained at  $20\text{ }^\circ\text{C}$  by circulating water. The clays used could be synthetic saponite  $[(\text{Na}_{0.25}\text{Mg}_{0.07})(\text{Mg}_{2.98}\text{Al}_{0.01})(\text{Si}_{3.6}\text{Al}_{0.4})\text{O}_{10}(\text{OH})_2]$  (denoted by SAP) or sodium montmorillonite  $[(\text{Na}_{0.25}\text{Mg}_{0.07})(\text{Al}_{1.56}\text{Mg}_{0.34}\text{Fe}_{0.10})(\text{Si}_{3.85}\text{Al}_{0.15})\text{O}_{10}(\text{OH})_2]$  (denoted by MON) or synthetic hectorite  $[\text{Na}_{0.46}(\text{Mg}_{2.62}\text{Li}_{0.46})\text{Si}_4\text{O}_{10}\text{F}_2]$ . A floating monolayer was formed at an air–water

interface by spreading a chloroform solution of an Ir(III) complex (*ca.*  $5.0 \times 10^{-5} \text{ mol L}^{-1}$ ) over an aqueous suspension of a clay ( $10 \text{ mg L}^{-1}$ ). The surface pressure versus molecular area ( $\pi$ -A) curves were obtained by compressing the monolayer. The deposition of the floating film onto a hydrophilic substrate was performed vertically.

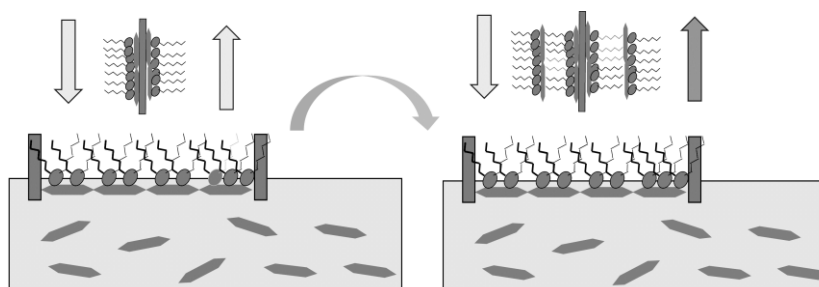
Figure 1 shows the examples of the  $\pi$ -A curves for DFPPY, PPY and PIQ, using  $10 \text{ mg L}^{-1}$  of SAP as a subphase. In all cases, surface pressure levels off from zero in the region of the molecular area below  $0.5\text{--}1.5 \text{ nm}^2$  per molecule. These facts supported the occurrence of hybridization of a molecular film of Ir(III) complex with clay particles at an air–water interface. After 30 min, the surface was compressed at a rate of  $10 \text{ cm}^2 \text{ min}^{-1}$  until the surface pressure reached  $10 \text{ mNm}^{-1}$ . Keeping the surface pressure at  $10 \text{ mNm}^{-1}$  for 30 min, the film was transferred onto a hydrophilic quartz plate (*ca.*  $1 \text{ cm} \times 2 \text{ cm} \times 1 \text{ mm}$ ) by the vertical deposition method at a dipping rate of  $10 \text{ mm min}^{-1}$ .

In order to prepare the mono-layered hybrid films containing a mixture of Ir(III) complexes, a mixture of two or three kinds of Ir (III) complexes in chloroform was spread over a suspension of clay. Double- or triple-layered films with different layer sequences were prepared by the layer-by-layer deposition method as shown in Scheme 2. In the procedures, quartz plates were dried in vacuum for 30 min after depositing each layer. The structural model of a prepared deposited film was schematically shown in Scheme 3. The surface morphology and layer structures were investigated by means of XRD and AFM measurements [39,66,67].

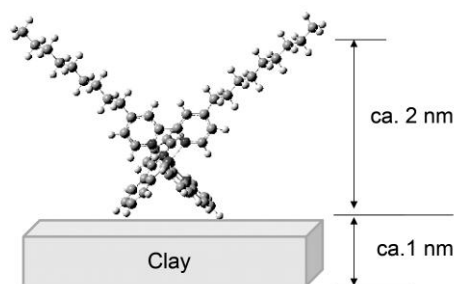
**Figure 1.** The  $\pi$ -A curves of (a) DFPPY, (b) PPY and (c) PIQ, using  $10 \text{ mgL}^{-1}$  of synthetic saponite as a subphase (modified from reference [67]).



**Scheme 2.** The layer-by-layer deposition method.



**Scheme 3.** Model of hybrid LB film: the possible structure in which a Ir(III) complex molecule, with the height of *ca.* 2.0 nm is adsorbed onto a single layer of clay whose thickness is *ca.* 1.0 nm(modified from reference [66]).



### 3. Photosensing of Gases by Hybrid LB Films

#### 3.1. Oxygen Photosensing by Hybrid Monolayered Films

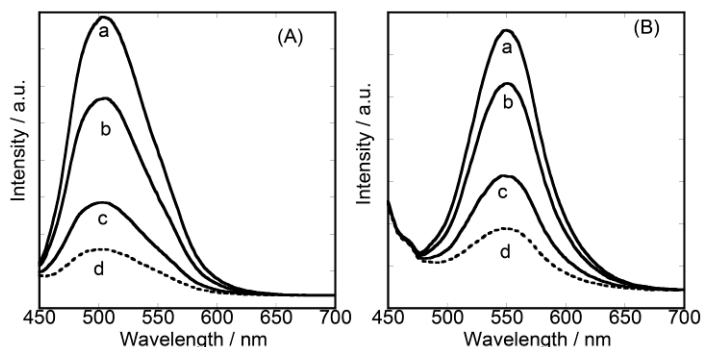
For the measurements of emission spectra from a deposited film, the surface-modified quartz plate was placed at 45 degrees with respect to the incident light in the quartz cell. The emitted light was detected at 90 degrees with respect to the incident light. The emission was measured either in vacuum (<0.1 kPa) or under oxygen atmosphere at room temperature.

Figure 2A,B shows the emission spectra, when a quartz substrate modified with {DFPPY/MON} or {PPY/MON} was irradiated at 430 nm, respectively. Measurements were performed under vacuum or oxygen atmosphere at room temperature. Emission peak wavelength ( $\lambda_{\text{max}}$ ) reflected the characters of each incorporated Ir(III) complex: that is,  $\lambda_{\text{max}} = 500$  nm and 550 nm for DFPPY and PPY, respectively. When an oxygen gas was introduced into the cell, the intensity of the emission decreased instantly due to the quenching of excited Ir(III) complexes by oxygen molecules. The Stern-Volmer plots are shown in Figure 3. The curves were fitted by the two-site model [66]. Comparing {PPY/MON} and {DFPPY/MON}, the latter exhibited more efficient quenching than the former. The change of emission intensity was record for {PPY/MON} and {DFPPY/MON}, when oxygen gas was introduced and evacuated. The films were irradiated at 430 nm and the emission was monitored at 500 nm and 550 nm, respectively. The rapid and reversible response was observed as shown in Figure 4. In case of {DFPPY/MON}, for example, more than 80% of the signal recovered to the initial level within 1 s on evacuating the oxygen gas. From the results on the single-layered hybrid films, it was concluded that a nanometer-thick film exhibited sufficiently high emission characteristic of an adsorbed Ir(III) complex.

#### 3.2. Dual-Emitting Properties of Double-Layered Films in Oxygen Sensing

The emission properties were studied on heterogeneous double-layered films. As shown in Figure 5, when a double-layered film, {DFPPY/MON/PPY/MON}, was irradiated at 430 nm, it showed the emission spectrum with the broad maximum around 500–550 nm. The band included the emissions both from DFPPY ( $\lambda_{\text{max}}$  at 500 nm) and PPY ( $\lambda_{\text{max}}$  at 550 nm). Thus energy transfer occurred to a negligible extent in this film [66].

**Figure 2.** The luminescence spectra from the single-layered hybrid LB films of (A) {DFPPY/MON} and (B) {PPY/MON}. The excitation wavelength was 430 nm. The vertical axis denotes the intensity of luminescence at an arbitrary unit. a: in vacuum, b: 4 kPa, c: 27 kPa, d: 101.3 kPa of oxygen pressure (modified from reference [66]).



**Figure 3.** Stern-Volmer plots for quenching by oxygen molecules (a) {DFPPY/MON} and (b) {PPY/MON}. Curves were calculated with two site model (modified from reference [66]).

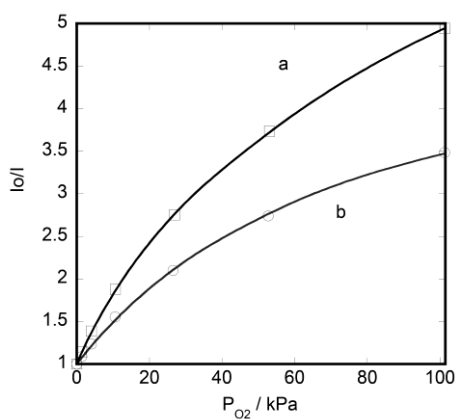
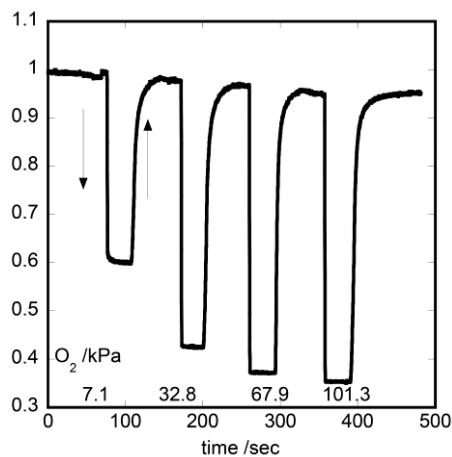


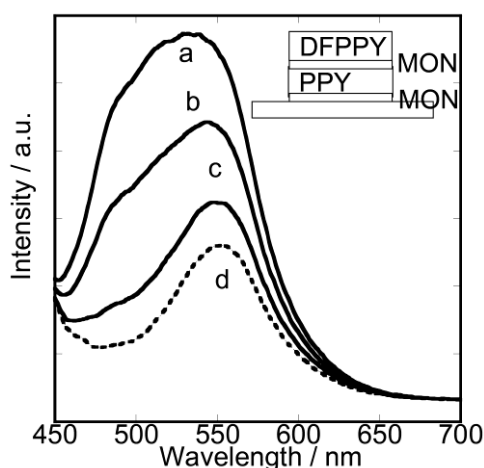
**Figure 4.** The change of emission intensity from {DFPPY/MON}, when oxygen gas was introduced and evacuated. The excitation and emission wavelengths were 430 nm and 500 nm at room temperature, respectively (modified from reference [66]).



One remarkable feature appeared in this film when oxygen gas was introduced. The spectral shape changed as a function of oxygen pressure (Figure 5). The film emitted light with the broad maximum around 500–550 nm at low oxygen pressure ( $0 < P_{O_2} < 4$  kPa), while the same film emitted light with the sharp maximum at 550 nm at high oxygen pressure ( $P_{O_2} > 4$  kPa). The observed dual properties were caused by the difference in quenching efficiency by oxygen molecules between DFPPY and PPY. That is, DFPPY was quenched efficiently more than PPY so that the former complex lost emitting capability more readily than the latter. The features confirmed the establishment of the strict layer-by-layer structures in the present hybrid films. These properties can be applied to develop an oxygen-sensing film whose emission spectrum changes depending on the pressure of oxygen gas.

The above results implied that oxygen molecules penetrated both the upper and lower layers, quenching the whole Ir(III) complexes in films. It was also confirmed that interlayer energy transfer took place between the metal complexes located in different layers.

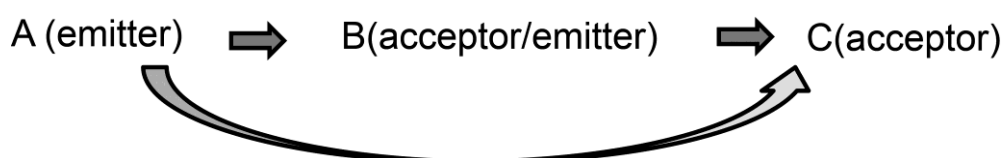
**Figure 5.** The luminescence spectra from the hetero-layered hybrid LB films of {DFPPY/MON/PPY/MON}. The excitation wavelength was 430 nm. The vertical axis denotes the intensity of luminescence at an arbitrary unit. a: in vacuum, b: 4 kPa, c: 27 kPa, d: 101.3 kPa of oxygen pressure (modified from reference [66]).



### 3.3. Unique Character of Triple-Layered Hybrid LB Films

The study of the emission properties was extended to a heterogeneous triple-layered film. Supposing that a film contains three kinds of emitters (denoted as A, B and C) in different layers, energy transfer might take place through the following three paths as shown in Scheme 4.

**Scheme 4.** Possible paths for energy transfer in a heterogeneous triple-layered film.



In case the rates of energy transfer in the above paths depend on the relative positions between an emitter and an acceptor, the total emission might be affected by the layer sequence. If oxygen

molecules quench these emitters, the effect might also depend on the layer sequence, since the efficiency might be affected by the penetration depth of an oxygen molecule in the film. As a result, two emitting molecules (A and B) located in different layers might be quenched to different degrees at a given pressure. Accordingly the contribution of each emitter to the total emission is dependent on oxygen pressure under a given layer sequence. These situations may lead to the appearance of multi-emission behavior, depending on the oxygen pressure.

Motivated by the above expectation, six triple-layered hybrid films with *different layer sequences* were prepared as shown in Scheme 5 [67]. The representative cases are shown in Figure 6 when the films were irradiated at 430 nm either under vacuum or at various oxygen pressures. In case of {DFPPY/SAP/PPY/SAP/PIQ/SAP}, the emission intensity decreased uniformly with no drastic change in the spectral shape. DFPPY\* in the uppermost layer was expected to be quenched most efficiently. The decrease of energy transfer from DFPPY\* resulted in the simultaneous lowering of emission from both PPY\* ( $\lambda_{\text{max}}$  at 550 nm) and PIQ\* ( $\lambda_{\text{max}}$  at 590 nm). In case of {PPY/SAP/DFPPY/SAP/PIQ/SAP}, however, the broad emission band (550–600 nm) changed to the sharp peak at 590 nm on increasing oxygen pressure. The emission intensity decreased with the increase of oxygen pressure until the emission peak remained around 590 nm. PPY\* in the uppermost layer was expected to be quenched more efficiently than PIQ\* in the lowest layer. Thus the emission from PIQ\* remained at higher oxygen pressure.

**Scheme 5.** Six kinds of triple-layered films with different layer sequences and mono-layered with mixed Ir(III) complexes. Here, {X/SAP} denotes the deposited layer of the hybrid film of an iridium(III) complex (X) with SAP, respectively (modified from reference [67]).

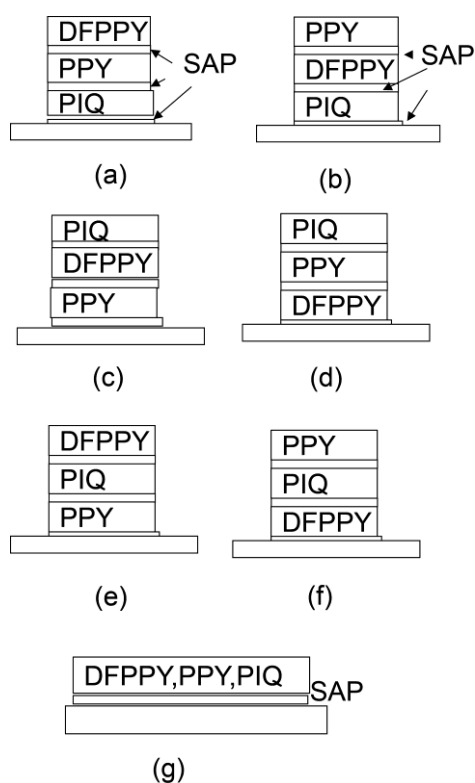
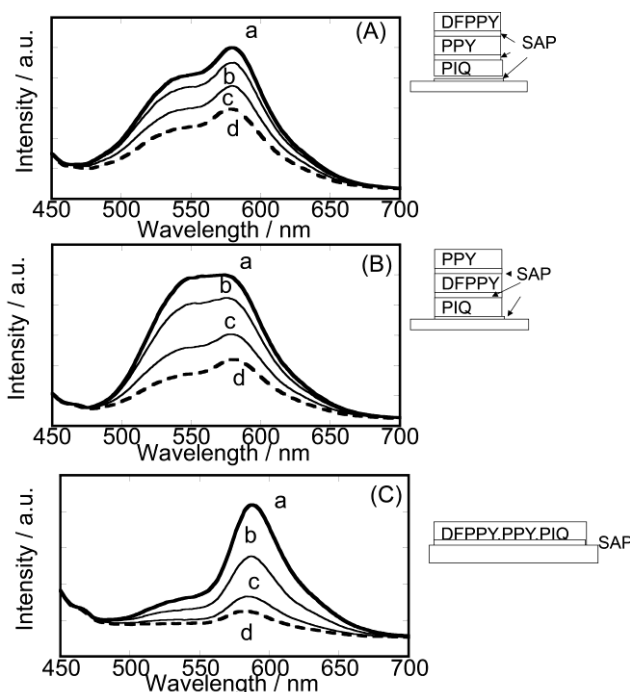


**Figure 6.** The luminescence spectra of the triple-layered hybrid LB films of (A) {DFPPY/SAP/PPY/SAP/PIQ/SAP}, (B) {PPY/SAP/DFPPY/SAP/PIQ/SAP}, (C) {DFPPY,PPY,PIQ/SAP}. The excitation wavelength was 430 nm. The vertical axis denotes the intensity of luminescence at an arbitrary unit. a: in vacuum, b: 4 kPa, c: 27 kPa, d: 101.3 kPa of oxygen pressure (modified from reference [67]).



The above results were contrasted with a single-layered film containing three kinds of Ir(III) complexes. In such a mixed film, PIQ emission alone was enhanced through energy transfer in the lateral direction from both PPY and DFPPY. The energy transfer took place from DFPPY to PPY, which was observed at shoulder of 520 nm. Increasing oxygen pressure, PPY was quenched and weak PIQ emission was observed.

#### 4. Perspective

The present hybrid films of clay nanosheets and photo-responsive iridium(III) complexes can be further extended to the following applications: (1) the development of more sensitive complexes would open the use of the films for rapid monitoring of oxygen molecules under extreme conditions, such as high or low temperature; (2) the multi-emitting character of multi-layered films may realize the visual monitoring of oxygen contents. Such monitoring is useful in the anti-oxidant polymer films of food preservation; and (3) the nanometer sized hybrid films might be used for patterning the distribution of oxygen molecules inside biological systems. These characters of clay nanosheets are unique in comparison with other inorganic hosts such as zeolite or mesoporous materials.

#### 5. Conclusions

The single- and multi-layered hybrid films of amphiphilic iridium(III) complexes with clay nanosheets were prepared according to the modified Langmuir-Blodgett (LB) method. In case of a

single-layered hybrid film, even a nanometer-thick film exhibited high emitting properties characteristic of an adsorbed molecule. Luminescence was monitored under the atmosphere of various gases. An oxygen gas, for example, quenched the emission from excited iridium(III) complexes linearly in the pressure range of 0–4 kPa, while the quenching effect was saturated above 4 kPa. Other gases with functional groups also quenched the luminescence efficiently. These results demonstrated the potential of the present hybrid LB films as a gas sensing device. For the mixed monolayer films, the intensity of red emission was enhanced due to the intra-layer energy transfer. For the double-layered films, the dual-emitting character was achieved due to the layer-by-layer deposition of  $[\text{Ir}(\text{dfppy})_2(\text{dc9bpy})]^+$  and  $[\text{Ir}(\text{ppy})_2(\text{dc9bpy})]^+$ . For the triple-layered films, one acceptor ( $[\text{Ir}(\text{piq})_2(\text{dc9bpy})]^+$ ) and two donor molecules ( $[\text{Ir}(\text{dfppy})_2(\text{dc9bpy})]^+$  and  $[\text{Ir}(\text{ppy})_2(\text{dc9bpy})]^+$ ) were separated in the different layers. The quenching efficiency by oxygen molecules was dependent on their penetrating depth in the films. As a result, oxygen molecules quenched these molecules in different ways under a given oxygen pressure. These conditions led to the appearance of multi-emission behavior. The present nanometer-thick films are regarded as a benchmark for an optical device emitting different visible lights in response to gas pressure.

### Acknowledgments

We thank the late Yasuhiko Nakatani, Kyoko Tsutumi, Yuji Kuniyoshi, Takeshi Odagiri and Miwa Ochi (Ehime University) for their preparation of the LB films and measurements. Thanks are also due to Kazuya Morimoto, Takahiro Nakae, Keishi Ohara, and Shin-ichi Nagaoka (Ehime University) for their valuable suggestions. This work has been financially supported by the JSPS KAKENHI Grant-Aid-for Scientific Research (B) Number 23350069, Grant-in-Aid for Exploratory Research Number 23655200 and Nippon Sheet Glass Foundation of Materials and Science and Engineering of Japan, JST A-STEP Number AS2421179M.

### Conflicts of Interest

The authors declare no conflict of interest.

### References

1. Balzani, V.; Juris, A.; Venturi, M.; Campagna, S.; Serroni, S. Luminescent and redox-active polynuclear transition metal complexes. *Chem. Rev.* **1996**, *96*, 759–833.
2. Wong, W.-Y.; Ho, C.-L. Heavy Metal organometallic electrophosphors derived from multi-component chromophores. *Coord. Chem. Rev.* **2009**, *253*, 1709–1968
3. Hasegawa, Y.; Nakagawa, T.; Kawai, T. Recent progress of luminescent metal complexes with photochromic units. *Coord. Chem. Rev.* **2010**, *254*, 2643–2651.
4. Chi, Y.; Chou, P.-T. Transition-metal phosphors with cyclometalating ligands: Fundamentals and applications. *Chem. Soc. Rev.* **2010**, *39*, 638–655.
5. Sato, H.; Yamagishi, A. Application of the  $\Delta\Lambda$  isomerism of octahedral metal complexes as a chiral source in photochemistry. *J. Photochem. Photobiol. C Photochem. Rev.* **2007**, *8*, 67–84.

6. King, K.A.; Spellane, P.J.; Watts, R.J. Excited-state properties of a triply ortho-metalated Iridium(III) complex. *J. Am. Chem. Soc.* **1985**, *107*, 1431–1432.
7. Tsuboyama, A.; Iwawaki, H.; Furugori, M.; Mukaide, T.; Kamatani, J.; Igawa, S.; Moriyama, T.; Miura, S.; Takiguchi, T.; Okada, S.; *et al.* Homoleptic Cyclometalated iridium complexes with highly efficient red phosphorescence and application to organic light-emitting diode. *J. Am. Chem. Soc.* **2003**, *125*, 12971–12979.
8. Tamayo, A.B.; Alleyne, B.D.; Djurovich, P.I.; Lamansky, S.; Tsyba, I.; Ho, N.N.; Bau, R.; Thompson, M.E. Synthesis and characterization of facial and meridional tris-cyclometalated iridium(III) complexes. *J. Am. Chem. Soc.* **2003**, *125*, 7377–7387.
9. Tamayo, A.B.; Garon, S.; Sajoto, T.; Djurovich, P.I.; Tsyba, I.M.; Bau, R.; Thompson, M.E. Cationic bis-cyclometalated iridium(III) diimine complexes and their use in efficient blue, green, and red electroluminescent devices. *Inorg. Chem.* **2005**, *44*, 8723–8732.
10. Sajoto, T.; Djurovich, P.I.; Tamayo, A.B.; Oxgaard, J.; Goddard, W.A., III; Thompson, M.E. Temperature dependence of blue phosphorescent cyclometalated Ir(III) complexes. *J. Am. Chem. Soc.* **2009**, *131*, 9813–9822.
11. Happ, B.; Winter, A.; Hager, M.D.; Schubert, U.S. Photogenerated avenues in macromolecules containing Re(I), Ru(II), Os(II), and Ir(III) metal complexes of pyridine-based ligands. *Chem. Soc. Rev.* **2012**, *41*, 2222–2255.
12. Zhao, J.; Ji, S.; Wu, W.; Wu, W.; Guo, H.; Sun, J.; Sum, H.; Liu, Y.; Li, Q.; Huang, L. Transition metal complexes with strong absorption of visible light and long-lived triplet excited States: From molecular design to applications. *RSC Adv.* **2012**, *2*, 1712–1728.
13. Zhou, G.; Wong, W.Y.; Yang, X. New design tactics in OLEDs using functionalized 2-phenylpyridine-type cyclometalates of iridium(III) and platinum(II). *Chem. Asian. J.* **2011**, *6*, 1706–1727.
14. Ladouceur, S.; Fortin, D.; Zysman-Colman, E. Role of substitution on the photophysical properties of 5,5'-Diaryl-2,2'-bipyridine (bpy\*) in [Ir(ppy)<sub>2</sub>(bpy\*)]PF<sub>6</sub> complexes: A combined experimental and theoretical study. *Inorg. Chem.* **2010**, *49*, 5625–5641.
15. Fischer, L.H.; Stich, M.I.J.; Wolfbeis, O.S.; Tian, N.; Holder, E.; Schäferling, M. Red- and green-emitting iridium(III) complexes for a dual barometric and temperature-sensitive paint. *Chem. Eur. J.* **2009**, *15*, 10857–10863.
16. Papkovsky, D.B.; Dmitriec, R.I. Biological detection by optical oxygen sensing. *Chem. Soc. Rev.* **2013**, *42*, 8700–8732.
17. Schäferling, M. The Art of fluorescence imaging with chemical sensors. *Angew. Chem. Int. Ed.* **2012**, *51*, 3532–3554.
18. Quaranta, M.; Borisov, S.M.; Klimant, I. Indicators for optical oxygen sensors. *Bioanal. Rev.* **2012**, *4*, 115–157.
19. Wolfbeis, O.S. Fiber-optic chemical sensors and biosensors. *Anal. Chem.* **2008**, *80*, 4269–4283.
20. Amao, Y. Probes and polymers for optical sensing of oxygen. *Microchim. Acta* **2003**, *143*, 1–12.
21. Sailor, M.J.; Wu, E.C. Photoluminescence-based sensing with porous silicon films, microparticles, and nanoparticles. *Adv. Funct. Mater.* **2009**, *19*, 3195–3208.
22. Ju, S.-Y.; Kopcha, W.P.; Papadimitrakopoulos, F. Brightly Fluorescent single-walled carbon nanotubes via an oxygen excluding surfactant organization. *Science* **2009**, *323*, 1319–1323.

23. Achatz, D.E.; Meier, R.J.; Fischer, L.H.; Wolfbeis, O.S. Luminescent sensing of oxygen using a quenchable probe and upconverting nanoparticles. *Angew. Chem. Int. Ed.* **2011**, *50*, 260–263.
24. Chu, C.-S.; Lo, Y.-L.; Sung, T.-W. Review on recent developments of fluorescent oxygen and carbon dioxide optical fiber sensors. *Photonic Sens.* **2011**, *1*, 234–250.
25. Lopez-Ruiz, N.; Martinez-Olmos, A.; de Vargas-Sansalvador, I.M.P.; Fernandez-Ramos, M.D.; Carvajal, M.A.; Capitan-Vallvey, L.F.; Palma, A.J. Determination of O<sub>2</sub> using colour sensing from image processing with mobile devices. *Sens. Actuators B* **2012**, *171–172*, 938–945.
26. Sotelo-Gonzalez, E.; Coto-Garcia, A.M.; Fernandez-Arguelles, M.T.; Costa-Fernandez, J.M.; Sanz-Medel, A. Immobilization of phosphorescent quantum dots in a sol–gel matrix for acetone sensing. *Sens. Actuators B* **2012**, *174*, 102–108.
27. Rothe, C.; Chiang, C.-J.; Jankus, V.; Abdullah, K.; Zeng, X.; Jitchati, R.; Batsanov, A.; Bryce, M.R.; Monkman, A.P. Ionic iridium(III) complexes with bulky side groups for use in light emitting cells: Reduction of concentration quenching. *Adv. Funct. Mater.* **2009**, *19*, 2038–2044.
28. Ulbricht, C.; Beyer, B.; Friebe, C.; Winter, A.; Schubert, U.S. Recent developments in the application of phosphorescent iridium(III) complex systems. *Adv. Mater.* **2009**, *21*, 4418–4441.
29. Guerchais, V.; Fillaut, J.-L. Sensory luminescent iridium(III) and platinum(II) complexes for cation recognition. *Coord. Chem. Rev.* **2011**, *255*, 2448–2457.
30. Lowry, M.S.; Bernhard, S. Synthetically tailored excited states: Phosphorescent, cyclometalated iridium(III) complexes and their applications. *Chem. Eur. J.* **2006**, *12*, 7970–7977.
31. Tian, N.; Lenkeit, D.; Pelz, S.; Fischer, L.H.; Escudero, D.; Schiewek, R.; Klink, D.; Schmitz, O.J.; Gomzález, L.; Schäferling, M.; *et al.* Structure–property relationship of red- and green-emitting iridium(III) complexes with respect to their temperature and oxygen sensitivity. *Eur. J. Inorg. Chem.* **2010**, *2010*, 4875–4885.
32. Xie, Z.; Ma, L.; deKrafft, K.E.; Jin, A.; Lin, W. Porous phosphorescent coordination polymers for oxygen sensing. *J. Am. Chem. Soc.* **2010**, *132*, 922–923.
33. DeRosa, M.C.; Mosher, P.J.; Yap, G.P.A.; Focsaneanu, K.-S.; Crutchley, R.J.; Evans, C.E.B. Synthesis, characterization, and evaluation of [Ir(ppy)<sub>2</sub>(vpy)Cl] as a polymer-bound oxygen sensor. *Inorg. Chem.* **2003**, *42*, 4864–4872.
34. DeRosa, M.C.; Hodgson, D.J.; Enright, G.D.; Dawson, B.; Evans, C.E.B.; Crutchley, R.J. Iridium luminophore complexes for unimolecular oxygen sensors. *J. Am. Chem. Soc.* **2004**, *126*, 7619–7626.
35. Clemente-León, M.; Coronado, E.; López-Muñoz, Á.; Repetto, D.; Ito, T.; Konya, T.; Yamase, T.; Constable, E.C.; Housecroft, C.E.; Doyle, K.; *et al.* Dual-emissive photoluminescent Langmuir–Blodgett films of decatungstoeuropate and an amphiphilic iridium complex. *Langmuir* **2010**, *26*, 1316–1324.
36. Bolink, H.J.; Baranoff, E.; Clemente-León, M.; Coronado, E.; Lardiés, N.; López-Muñoz, A.; Repetto, D.; Nazeeruddin, M.K. Dual-emitting Langmuir–Blodgett film-based organic light-emitting diode. *Langmuir* **2010**, *26*, 11461–11468.
37. Roldán-Carmona, C.; González-Delgado, A.M.; Guerrero-Martínez, A.; de Cola, L.; Giner-Casares, J.J.; Pérez-Morales, M.; Martín-Romero, M.T.; Camacho, L. Molecular organization and effective energy transfer in iridium metallosurfactant–porphyrin assemblies embedded in Langmuir–Schaefer films. *Phys. Chem. Chem. Phys.* **2011**, *13*, 2834–2841.

38. Sato, H.; Tamura, K.; Taniguchi, M.; Yamagishi, A. Highly luminescent Langmuir–Blodgett films of amphiphilic Ir(III) complexes for application in gas sensing. *New J. Chem.* **2010**, *34*, 617–622.
39. Sato, H.; Tamura, K.; Ohara, K.; Nagaoka, S.; Yamagishi, A. Hybridization of clay minerals with the floating film of a cationic Ir(III) complex at an air–water interface. *New J. Chem.* **2011**, *35*, 394–399.
40. Borisov, S.M.; Klimant, I. Ultrabright Oxygen optodes based on cyclometalated iridium(III) coumarin complexes. *Anal. Chem.* **2007**, *79*, 7501–7509.
41. Mak, C.S.K.; Pentlehner, D.; Stich, M.; Wolfbeis, O.S.; Chan, W.K.; Yersin, H. Exceptional oxygen sensing capabilities and triplet state properties of Ir(ppy-NPh<sub>2</sub>)<sub>3</sub>. *Chem. Mater.* **2009**, *21*, 2173–2175.
42. Toro, M.M.-S.; Fernández-Sánchez, J.F.; Baranoff, E.; Nazeeruddin, M.K.; Graetzela, M.; Fernandez-Gutierrez, A. Novel luminescent Ir(III) dyes for developing highly sensitive oxygen sensing films. *Talanta* **2010**, *82*, 620–626.
43. Medina-Castillo, A.L.; Fernández-Sánchez, J.F.; Klein, C.; Nazeeruddin, M.K.; Segura-Carretero, A.; Fernández-Gutiérrez, A.; Graetzel, M.; Spichinger-Keller, U.E. Engineering of efficient phosphorescent iridium cationic complex for developing oxygen-sensitive polymeric and nanostructured films. *Analyst* **2007**, *132*, 929–936.
44. Marín-Suárez, M.; Curchod, B.F.E.; Tavernelli, I.; Rothlisberger, U.; Scopelliti, R.; Jung, I.; Di Censo, D.; Grätzel, M.; Fernández-Sánchez, J.F.; Fernández-Gutiérrez, A.; *et al.* Nanocomposites containing neutral blue emitting cyclometalated iridium(III) emitters for oxygen sensing. *Chem. Mater.* **2012**, *24*, 2330–2338.
45. Medina-Rodríguez, S.; Marín-Suárez, M.; Fernández-Sánchez, J.-F.; de la Torre-Vega, Á.; Baranoff, E.; Fernández-Gutiérrez, A. High performance optical sensing nanocomposites for low and ultra-low oxygen concentrations using phase-shift measurements. *Analyst* **2013**, *138*, 4607–4617.
46. Aiello, D.; Talarico, A.M.; Teocoli, F.; Szerb, E.I.; Aiello, I.; Testa, F.; Ghedini, M. Self-incorporation of a luminescent neutral iridium(III) complex in different mesoporous micelle-templated silicas. *New J. Chem.* **2011**, *35*, 141–148.
47. Mori, K.; Tottori, M.; Watanabe, K.; Che, M.; Yamashita, H. Photoinduced aerobic oxidation driven by phosphorescence Ir(III) complex anchored to mesoporous silica. *J. Phys. Chem. C* **2011**, *115*, 21358–21362.
48. Waki, M.; Mizoshita, N.; Tani, T.; Inagaki, S. Periodic mesoporous organosilica derivatives bearing a high density of metal complexes on pore surfaces. *Angew. Chem. Int. Ed.* **2011**, *50*, 11667–11671.
49. Machizuki, D.; Sugiyama, M.; Maitani, M.M.; Wada, Y. Rigidochromic phosphorescence of [Ir(2-phenylpyridine)<sub>2</sub>(2,2'-bipyridine)]<sub>+</sub> in C16TMA<sup>+</sup>: Layered silicate and its Förster resonance energy transfer. *Eur. J. Inorg. Chem.* **2013**, *2013*, 2324–2329.
50. Sato, H.; Tamura, K.; Taniguchi, M.; Yamagishi, A. Metal ion sensing by luminescence from an ion-exchange adduct of clay and cationic cyclometalated iridium(III) complex. *Chem. Lett.* **2009**, *38*, 14–15.

51. Sato, H.; Tamura, K.; Aoki, R.; Kato, M.; Yamagishi, A. Enantioselective sensing by luminescence from cyclometalated iridium(III) complexes adsorbed on a colloidal saponite clay. *Chem. Lett.* **2011**, *40*, 63–65.
52. Hussain, S.A.; Chakraborty, S.; Bhattacharjee, D.; Schoonheydt, R.A. Fluorescence resonance energy transfer between organic dyes adsorbed onto nano-clay and Langmuir–Blodgett (LB) films. *Spectrochim. Acta Part A* **2010**, *75*, 664–667.
53. Shichi, T.; Takagi, K. Clay minerals as photochemical reaction fields. *J. Photochem. Photobiol. C Photochem. Rev.* **2000**, *1*, 113–130.
54. Ogawa, M.; Kuroda, K. Photofunctions of intercalation compounds. *Chem. Rev.* **1995**, *95*, 399–438.
55. Sato, H.; Hiroe, Y.; Tamura, K.; Yamagishi, A. Orientation tuning of a polypyridyl Ru(II) complex immobilized on a clay surface toward chiral discrimination. *J. Phys. Chem. B* **2005**, *109*, 18935–18941.
56. Sasai, R.; Itoh, T.; Ohmori, W.; Itoh, H.; Kusunoki, M. Preparation and characterization of Rhodamine 6G/alkyltrimethylammonium/laponite hybrid solid materials with higher emission quantum yield. *J. Phys. Chem. C* **2009**, *113*, 415–421.
57. Umemura, Y.; Yamagishi, A.; Schoonheydt, R.; Persoons, A.; de Schryver, F. Langmuir–Blodgett films of a clay mineral and Ruthenium(II) complexes with a noncentrosymmetric structure. *J. Am. Chem. Soc.* **2002**, *124*, 992–997.
58. Shimada, T.; Yamada, H.; Umemura, Y. Surface potential studies on adsorption processes of clay nanosheets onto a floating molecular film of an amphiphilic alkylammonium cation. *J. Phys. Chem. B* **2012**, *116*, 4484–4491.
59. Ishida, Y.; Shimada, T.; Masui, D.; Tachibana, H.; Inoue, H.; Takagi, S. Efficient excited energy transfer reaction in clay/porphyrin complex toward an artificial light-harvesting system. *J. Am. Chem. Soc.* **2011**, *133*, 14280–14286.
60. Ishida, Y.; Masui, D.; Tachibana, H.; Inoue, H.; Shimada, T.; Takagi, S. Controlling the microadsorption structure of porphyrin dye assembly on clay surfaces using the “Size-Matching Rule” for constructing an efficient energy transfer system. *ACS Appl. Mater. Interfaces* **2012**, *4*, 811–816.
61. Ishida, Y.; Masui, D.; Shimada, T.; Tachibana, H.; Inoue, H.; Takagi, S. The mechanism of the porphyrin spectral shift on inorganic nanosheets: The molecular flattening induced by the strong host–guest interaction due to the “Size-Matching Rule”. *J. Phys. Chem. C* **2012**, *116*, 7879–7885.
62. Ishida, Y.; Shimada, T.; Tachibana, H.; Inoue, H.; Takagi, S. Regulation of the collisional self-quenching of fluorescence in clay/porphyrin complex by strong host–guest interaction. *J. Phys. Chem. A* **2012**, *116*, 12065–12072.
63. Takagi, S.; Tryk, D.A.; Inoue, H. Photochemical energy transfer of cationic porphyrin complexes on clay surface. *J. Phys. Chem. B* **2002**, *106*, 5455–5460.
64. Takagi, S.; Eguchi, M.; Tryk, D.A.; Inoue, H. Light-harvesting energy transfer and subsequent electron transfer of cationic porphyrin complexes on clay surfaces. *Langmuir* **2006**, *22*, 1406–1408.
65. Čeklovský, A.; Takagi, S. Oxygen sensing materials based on clay/metalloporphyrin hybrid systems. *Org. Eur. J. Chem.* **2013**, *11*, 1132–1135.

66. Morimoto, K.; Nakae, T.; Ohara, K.; Tamura, K.; Nagaoka, S.; Sato, H. Dual emitting Langmuir—Blodgett films of cationic iridium complexes and montmorillonite clay for oxygen sensing. *New. J. Chem.* **2012**, *36*, 2467–2471.
67. Sato, H.; Tamura, K.; Ohara, K.; Nagaoka, S. Multi-emitting properties of hybrid Langmuir-Blodgett films of amphiphilic iridium complexes and the exfoliated nanosheets of saponite clay. *New. J. Chem.* **2013**, *38*, doi:10.1039/C3NJ00879G.
68. Sato, H.; Tamura, A.; Yamagishi, A. Application of Clay Mineral-Iridium(III) Complexes Hybrid Langmuir-Blodgett Films for Photosensing. In *Clay Minerals in Nature*, 1st ed.; Valášková, M., Martynková, G.S., Eds.; Intechopen. Com.: Rijeka, Croatia, 2012; pp. 259–272.
69. Inukai, K.; Hotta, Y.; Taniguchi, M.; Tomura, S.; Yamagishi, A. Formation of a clay monolayer at an air-water interface. *J. Chem. Soc. Chem. Commun.* **1994**, doi:10.1039/C39940000959.

© 2014 by the authors; licensee MDPI, Basel, Switzerland. This article is an open access article distributed under the terms and conditions of the Creative Commons Attribution license (<http://creativecommons.org/licenses/by/3.0/>).